

## 7.4 First Observation of the Fourth Neutral Polarization Point in the Atmosphere

### 7.4.1 The Last Neutral Point of Atmospheric Polarization

In the clear sunlit normal sky there exist only three loci, the Arago, Babinet and Brewster neutral points, where the skylight is unpolarized (Können 1985). The antecedents date back to 1809 when the French astronomer Dominique Francois Jean Arago discovered the partial linear polarization of skylight, and soon thereafter, above the antisun he observed a neutral point which nowadays bears his name (see Barral 1858). In 1840 the French meteorologist Jacques Babinet discovered a second neutral point situated above the sun (Babinet 1840). Since a neutral point existed above the sun, from considerations of symmetry, the Scottish physicist David Brewster predicted a third point of zero degree of polarization positioned at a similar angular distance below the sun along the solar meridian. This celestial point, called nowadays the Brewster neutral point, was found later at the theoretically predicted position (Brewster 1842). Only in 1846 could confirm Babinet the existence of the Brewster point (Brewster 1847).

Figures 7.4.1A and 7.4.1B show the relative positions of the Arago, Babinet and Brewster neutral points in the sky. Occasionally, some secondary neutral points have also been observed under special conditions associated with reflections from water surfaces (Brewster 1847; Soret 1888), turbid atmospheres after volcanic eruptions (Cornu 1884), or total solar eclipses (Pomozi et al. 2001a; Horváth et al. 2003).

With Brewster's discovery, the three principal neutral points, and the only ones now bearing the names of their discoverers, were known. They have been the subject of many ground-based investigations since their first observation, because their positions have been proven to be sensitive indicators of the amount and type of atmospheric turbidity (Coulson 1988). In the second half of the 20th century, however, the neutral points have lost their importance in applied meteorology and became a neglected tool in meteorological research (Neuberger 1950).

Theoretically, for reasons of symmetry, a fourth neutral point should exist below the antisun (Fig. 7.4.1). However, it cannot be observed from the ground, because the region below the antisolar point is either under the horizon after sunrise (Figs. 7.4.1A,B), or after sunset it is in the shadow of the earth (Fig. 7.4.1C) thus the sub-antisolar region is not illuminated by direct sunlight, which is the prerequisite of the occurrence of the fourth neutral point. The fourth neutral point can be observed only in the sunlit atmosphere and at appropriately high altitudes in the air (Fig. 7.4.1E) or space (Fig. 7.4.1F) somewhere below the antisun. The light field in the atmosphere can be divided into two components (Fig. 7.4.1):

1. The radiation scattered downward to the earth's surface (downwelling light field) from the sunlit sky is called "skylight".
2. The radiation directed to space (upwelling light field) and originating from scattering of sunlight in the atmosphere and reflection of light from the earth's surface is termed "earthlight" (Coulson 1988).

For a ground-based observer, the Arago, Babinet and Brewster points are the neutral points of polarized skylight scattered downward to the surface of the earth (Figs. 7.4.1A,B). For an air- or space-borne observer the Brewster point and the fourth neutral point result from the upward scattering of sunlight within the atmosphere and from the reflection of sunlight from the surface of the earth (Figs. 7.4.1E,F).

Before 2001, no observation of the fourth neutral point has been reported and so it has remained nameless. Apparently, the fourth neutral point has been overlooked in observational atmospheric optics, even though theoretical considerations (e.g. Rozenberg 1966) or model computations (Bréon et al. 1997) have predicted its existence. It has been mentioned only occasionally in the literature. Rozenberg (1966), for example, called it the "point observable from above", but it is not even mentioned in the most famous monographs on polarized light in nature (Gehrels 1974; Können 1985; Coulson 1988). Until 2001, this anonymous "fourth" neutral point has not been observed during air- or space-borne polarimetric experiments (e.g. Rao 1969; Coulson et al. 1986; Herman et al. 1986; Deuzé et al. 1989, 1993; Deschamps et al. 1994) and has been forgotten, despite that the neutral points were a basic tool in atmospheric research for a century (Neuberger 1950).

With this in mind, Horváth et al. (2002b) (Fig. 7.4.7D) performed two hot air balloon flights over Hungary immediately after sunrise. Using 180° field-of-view imaging polarimetry, they measured the patterns of the degree  $p$  and angle  $\alpha$  of linear polarization of earthlight in the red (650 nm), green (550 nm) and blue (450 nm) parts of the spectrum below the balloon's gondola as functions of the altitude and solar elevation. This technique has been proven to be an effective tool for the quantitative study of neutral points (Gál et al. 2001a,b,c; Pomozi et al. 2001a,b; Horváth et al. 2002a,b, 2003).

The aim of the first flight of Horváth et al. (2002b) was to test the measuring apparatus onboard and to check whether the 4000 m operational ceiling of the hot air balloon is enough to observe the fourth neutral point during and immediately after sunrise when the cloudless atmosphere is illuminated by approximately horizontally directed sunlight, which situation is ideal for this observation. The first flight was successful and Horváth et al. (2002b) were able as first to observe the fourth neutral point at different altitudes between 2000 and 3500 m. Then they performed a second flight to determine the lowest altitude, at which the fourth neutral point can be still observed.

#### 7.4.2 Conditions of the Hot Air Balloon Flights to Observe the Fourth Neutral Point

Horváth et al. (2002b) conducted the two flights with a hot air balloon of the Hungarian Airlines Aero Club (MALÉV, Budapest). The operational ceiling of hot air balloons without oxygen-masks for the crew is 4000 m above the ground level. The flights and measurements were performed with the following crews:

- Gábor Horváth (group leader), Balázs Bernáth (Ph.D. student), Bence Suhai (undergraduate student) and Attila Bakos (pilot) on 28 June 2001 at local sunrise 04:52 (= local summer time = UTC+2);
- Gábor Horváth, Balázs Bernáth, András Barta (Ph.D. student) and Attila Bakos on 25 August 2001 at local sunrise 05:56.

In both cases the balloon launched prior to the local sunrise from the immediate vicinity of the Hungarian town Pákozd (47°13'N, 18°33'E). Horváth et al. (2002b) chose this time for launching, because at sunrise and sunset the contribution of light reflected from the ground is small to the earthlight which is dominated by atmospheric light scattering, especially for shorter (UV, blue) wavelengths. Furthermore, at sunrise and sunset the antisun has a minimal (zero) elevation resulting in a maximal distance between the aerial observer and the earth's surface in the predicted direction of the fourth neutral point (about 20°-35° below the antisun).

The first prerequisite of observation of the fourth neutral point is an appropriately thick air layer below the antisun in which the sunlight can be backscattered towards the aerial observer (Fig. 7.4.1E). The second prerequisite is that this backscattered light must not be suppressed by the ground-reflected light. Thus, the sunrise and sunset are ideal periods to observe the fourth neutral point. Depending on the meteorological conditions, a hot air balloon can climb to 4000 m within about 15-20 minutes, and to lose its height up to the ground needs about 20-25 minutes. Since hot air balloons must stay grounded from sunset until sunrise, and safe landing require good visibility, one could not measure the polarization pattern of earthlight at sunset at high altitude. This is the reason why Horváth et al. (2002b) measured at sunrise.

During the first flight the balloon drifted slowly toward south-east and landed in the immediate vicinity of the town Adony (47°06'N, 18°51'E), while during the second flight the balloon hovered approximately above Pákozd due to calm weather conditions at the relatively low (below 1400 m) altitudes of this flight. Figure 7.4.2A shows the trajectory of the balloon on the map of Hungary during the first flight. In Fig. 7.4.2B the altitude of the balloon is seen as a function of time after sunrise for both flights. The altitudes and the points of time at which polarimetric measurements were done are represented by small black-filled triangles in the two plots of Fig. 7.4.2B.

During the first flight, the minimum and maximum altitude at which the polarization pattern of earthlight was measured was 2000 and 3500 m. During the second flight measurements were performed when the balloon hovered between

800 and 1400 m. Figure 7.4.2C shows the solar elevation versus the time after sunrise derived for the ground from the latitude and longitude of the launching site at Pákozd and from the time of measurements. The dependence of the solar elevation on the change of the balloon's longitude and latitude (during the first flight) as well as altitude (during both flights) was negligible.

During both flights the atmosphere was slightly hazy but cloudless, the rising sun was not occluded by distant clouds. At Pákozd (launching site) and between Pákozd and Adony (landing site), the ground surface was a mixture of areas which are typical for agricultural cultivation: green grass-land, fields, meadows, plough-land with a mosaic pattern of different albedos. Near Pákozd there is lake Velence partly occupied by areas of green reed and reed-grass. During the second flight in some places there was a thin (2-5 m) fog layer immediately above the ground surface.

#### **7.4.3 Measurement of the Polarization Patterns of Earthlight by 180° Field-of-View Imaging Polarimetry**

The objective was to measure the degree and angle of linear polarization of the upwelling earthlight in the whole terrestrial hemisphere. For this purpose a 180° field-of-view, rotating-analyzer imaging photopolarimeter was used (Gál et al. 2001c). The down-facing polarimeter was mounted onto a holder which hung on the outside of the gondola. The holder made it possible to slide up and down the polarimeter vertically. The verticality of the optical axis of the fisheye lens was checked by two orthogonal water levels on the camera and ensured by appropriate adjustments of the holder. Performing the measurements in the tiny gondola of the balloon required strict choreography. One measurement section happened in the following way:

1. Leaning out cautiously from the gondola, and after setting the time of exposure and the aperture of the camera, the first member of the crew (G. Horváth) let down the polarimeter below the bottom level of the gondola.
2. Squating in one of the corners of the gondola, the second member of the crew (B. Bernáth) reached out with one of its arms through an opening of the gondola to expose and turn away the filter wheel of the polarimeter three times, which lasted about 6 s.
3. Then the first person lifted the polarimeter, reset the time of exposure and the aperture, and let down again the polarimeter.
4. In the meantime, the third member of the crew (B. Suhai or A. Barta) took a note of the time of measurement, the aperture, the time of exposure and the altitude of the balloon. The fourth member of the crew was the pilot (A. Bakos) of the hot air balloon.

During the evaluation of the three polarizational pictures the following problem arose from the aerial manner of the measurements from the gondola: During the 6 s of one measurement the gondola drifted a little and turned away sometimes,

which resulted in more or less translations and rotations of the corresponding pixels of the three pictures relative to each other. The small spatial disparities (shifts) between the corresponding pixels induced by the drift caused small motion artefacts only in the polarization patterns of the ground surface, but did not affect those of the atmospheric light scattering. This is well seen in Figs. 7.4.3H,I,J, for example, where in the red spectral range small motion artefacts occur, which disappear in the blue part of the spectrum (Figs. 7.4.3B,C,D). However, the rotation of the corresponding pixels around the nadir due to the rotation of the gondola during the measurements must have been compensated in many cases. This was performed in such a way that at a given triplet of the digitized polarizational pictures, every picture was rotated around the nadir until some special selected common points of the pictures (small bright spots, road intersections, or the edges and angles of bright regions of the ground surface) coincided with a pixel accuracy.

#### 7.4.4 Control Measurement of the Polarization Patterns of the Full Sky at Sunrise

The polarization patterns of the full sky was measured by the same 180° field-of-view imaging polarimeter as those of the earthlight from the gondola of the hot air balloon. The skylight measurement was performed from the ground on 26 August 1999 at local sunrise (06:00 = local summer time = UTC+1, solar elevation = 0°) in the Tunisian salt pan Chott el Djerid, 10 km from Kriz (33°52'N, 8°22'E) as described by Pomozi et al. (2001b). The desert ground was flat reddish/yellowish sand. The measured polarization patterns of skylight served as a control for comparison with the polarization distribution of earthlight and the Arago and Babinet neutral points of skylight polarization, which are not visible on the earthlight patterns.

#### 7.4.5 Characteristics of the Fourth Neutral Point

Figure 7.4.3 shows the patterns of radiance  $I$ , degree  $p$  and angle  $\alpha$  of linear polarization of earthlight measured by 180° field-of-view imaging polarimetry at an altitude of 3500 m immediately after sunrise at a solar elevation of 2° in the red (650 nm), green (550 nm) and blue (450 nm) spectral ranges during the first flight on 28 June 2001. In the  $p$ -patterns (Figs. 7.4.3C,F,I) two neutral points are clearly discernible in all three spectral ranges: the neutral point located along the solar meridian is the Brewster point, and the other along the antisolar meridian is the fourth neutral point. At both neutral points  $p = 0$ , and moving off them  $p$  gradually increases. In Figs. 7.4.3C,F,I low  $p$ -values are coded by blue, green and yellow colours, and the neutral points are positioned in the centre of two regions of very low  $p$ . These weakly polarized areas are the most compact in the blue, and are the most diffuse in the red.

The reason for this is that the longer the wavelength, the greater is the contribution of ground-reflected light to the earthlight. The neutral points are the result of higher order scattering of sunlight in the atmosphere, and due to the Rayleigh law these higher order scattering events dominate at shorter (UV and blue) wavelengths over ground reflection. At longer wavelengths the intensity of atmospheric scattering decreases and the relative influence of ground reflection increases as can be well seen in the *I*-patterns (Figs. 7.4.3B,E,H). This can also be seen in the *p*-patterns: in the blue *p* of earthlight changes smoothly and gradually as a function of the direction of view, while in the red *p* changes suddenly at the edges of neighbouring dark and bright regions of the ground.

In the  $\alpha$ -patterns of Fig. 7.4.3 we see that both neutral points are positioned along the so-called "neutral lines", coinciding with the border line between the eight-shaped blue/green regions and the yellow/red areas, along which  $\alpha = \pm 45^\circ$  or  $\pm 135^\circ$  (Stokes parameter  $Q = 0$ ). Generally, *p* is not equal to zero at neutral lines except as they intersect the solar and antisolar meridian at the neutral points, where  $p = 0$ . On the other hand, crossing the neutral points along the solar or antisolar meridian,  $\alpha$  has a sudden change of  $90^\circ$ , because the polarization switches from "positive" (shaded with bright green and blue in the  $\alpha$ -patterns, and meaning direction of polarization perpendicular to the scattering plane determined by the observer, the sun and the point observed) to "negative" (shaded with bright red and yellow, and meaning direction of polarization parallel to the scattering plane). Also in the  $\alpha$ -patterns we can see the increasing disturbing effect of ground-reflected light as the wavelength increases.

The nadir angles of the Brewster and fourth neutral points determined on the basis of the *p*- and  $\alpha$ -patterns of Fig. 7.4.3 are seen in Table 7.4.1. The general trend is that the shorter the wavelength, the closer are located the neutral points to the nadir, which phenomenon is explained below. Horváth et al. (2002b) evaluated also several other imaging polarimetric measurements done at different altitudes between 2000 and 3500 m during their first flight, and obtained similar results as shown in Fig. 7.4.3: in all of these *p*- and  $\alpha$ -patterns the fourth neutral point as well as the Brewster point were visible in all three spectral ranges.

The aim of the second hot air balloon flight conducted on 25 August 2001 during and immediately after sunrise was to estimate the lowest altitude, at which the fourth neutral point can be still observed. At an altitude of 900 m and at a solar elevation of  $3^\circ$  the fourth neutral point could still be discerned in the polarization patterns measured in the blue and green. In the red the area of very low *p* around the theoretical position of the fourth neutral point was very diffuse, and only the Brewster point could be clearly observed in the *p*- and  $\alpha$ -patterns. Due to the low altitude, in the red the disturbing effect of ground reflection was so great and the relative contribution of atmospheric scattering to the earthlight was so small that the fourth neutral point was not clearly seen yet. Nevertheless, in the red there was a local minimum of *p* at the predicted position of the fourth neutral point. Under the meteorological conditions during the second flight the lower limit of the altitude was about 900 m at which the fourth neutral point could be observed.

In order to compare the polarization patterns of earthlight measured at near zero solar elevations at sunrise with those of skylight when the sun is on the horizon, in Fig. 7.4.4 the polarization patterns of skylight, measured by 180° field-of-view imaging polarimetry from the ground at 650, 550 and 450 nm on 26 August 1999 at sunrise in the Tunisian salt pan Chott el Djerid, are presented. Comparing Fig. 7.4.3 with Fig. 7.4.4, a great similarity between the polarization patterns can be established. In all polarization patterns of Fig. 7.4.4 the Arago and Babinet points are clearly discernible, and these patterns possess similar qualitative features as those in Fig. 7.4.3. There are, of course, some quantitative differences between the polarization patterns of earthlight and skylight:

- At given angles from the solar meridian and the nadir/zenith,  $p$  of skylight is much higher than that of earthlight.
- The neutral points of skylight polarization are located at greater angular distances from the zenith than those of earthlight from the nadir (see Table 7.4.1).
- The change of polarization versus direction of view is smoother in the skylight patterns than it is in the earthlight patterns.

One reason for these differences is that the polarization of skylight observed from the ground is the result of scattering of sunlight within the whole atmosphere, while the air layer below the balloon comprises only part of the earth's atmosphere. Another reason is that skylight has only one component (downwelling scattered light), while earthlight is the combination of light backscattered by the atmosphere and light reflected from the ground, the latter influencing strongly the upwelling radiation field.

Figures 7.4.5 and 7.4.6 show  $p$  and  $\alpha$  of earthlight and skylight along the solar and antisolar meridian measured at 650, 550 and 450 nm as a function of the viewing angle  $\theta$  from the nadir or zenith. These data for the earthlight and skylight originate from the polarization patterns in Figs. 7.4.3 and 7.4.4, respectively. In the plots of Fig. 7.4.5, the local minima  $p = 0$  at the neutral points and the maxima of  $p$  at the nadir/zenith are clearly visible. The maximum of  $p$  of earthlight is about the half or third of that of skylight due to the depolarizing effect of light reflected from the ground and multiply scattered on aerosols. The slight haze in the atmosphere during the balloon-borne measurements enhanced multiple scattering of the first component of earthlight, the sunlight scattered by aerosols (Bohren 1987), which resulted in a reduction of  $p$  of earthlight (Figs. 7.4.5A,C,E) and an increase of the area of negative polarization (Figs. 7.4.6A,C,E). The latter effect decreased the nadir angle of the Brewster and fourth neutral points (Table 7.4.1). The second component of earthlight, the sunlight reflected diffusely from the rough terrain, suffered also depolarization, which also decreased  $p$  of earthlight, especially at longer (green and red) wavelengths. These effects explain why earthlight was less polarized than skylight above the arid Tunisian desert, and why the Arago and Babinet points of skylight polarization in Tunisia were nearer the horizon than the Brewster and fourth neutral points of earthlight polarization.

In Fig. 7.4.6 we can see that along the solar and antisolar meridian,  $\alpha$  of both earthlight and skylight is always approximately  $90^\circ$  (perpendicular to the scattering plane, which means positive polarization) between the (fourth and Brewster as well as Arago and Babinet) neutral points, and passing the neutral points,  $\alpha$  switches to approximately  $0^\circ$  and  $180^\circ$  (parallel to the scattering plane, which means negative polarization). The noise of the measured  $\alpha$ -values is maximal at and near the neutral points due to the very low degrees of polarization. In Figs. 7.4.5 and 7.4.6 the noise of both the  $p$ - and  $\alpha$ -plots of earthlight gradually increases from the short (blue) wavelengths to the long (red) ones because of the increasing influence of ground-reflected light. Figures 7.4.7A-C, summarizing the essence of the balloon-borne measurements, show the three-dimensional distribution of polarization as well as the Arago and fourth neutral points observable around a hot air balloon in the blue (450 nm) spectral range at an altitude of 3500 m.

#### 7.4.6. Origin and Characteristics of the Principal Neutral Points

In the clear atmosphere, a neutral point occurs if the radiance of the normally positively polarized sky- or earthlight is matched exactly by an equal quantity of negatively polarized light. Multiple scattering of light by dust, haze and other aerosol particles in the atmosphere introduce positive or negative polarization, depending on characteristics of the particles and the incident radiation. Under clear atmospheric conditions, multiple scattering causes more negative polarization than positive one, thus the net  $p$  of skylight is reduced. The stronger the multiple scattering, the more negative polarization is introduced in the atmosphere, and the more the neutral points are displaced from the sun or antisun. The amount of multiple scattering is strongly affected by atmospheric turbidity.

The different angular positions of the neutral points observed in the red, green and blue ranges of the spectrum (Figs. 7.3.1, 7.4.3, 7.4.4, Table 7.4.1) are the consequence of the dispersion of polarization, the influence of wavelength-dependent ground reflection and the spectral composition of direct sunlight. Under normal, clear atmospheric conditions and when the atmosphere is illuminated by sunlight (for higher solar elevations from the horizon) and the ground reflection is approximately independent of wavelength (for colourless grounds covered by snow or grey/white sand, black soil, for example), a general rule is that the shorter the wavelength of light, the lower the degree of skylight polarization (Coulson 1988). There is little spectral dependency at wavelengths  $\lambda > 500$  nm, but strong dispersion for shorter wavelengths. The strong decrease of  $p$  towards shorter wavelengths is due mainly to multiple scattering, because  $p$  resulting from a single scattering event is independent of wavelength. At shorter wavelengths multiple scattering reduces  $p$ , increasing the magnitude of negative polarization and thus shifting the positions of the neutral points further away from the sun or antisun.

Thus, the region of negative polarization surrounding the sun and antisun is much more extended in the short-wavelength (UV and blue) than in the long-wavelength (green and red) range of the spectrum. This is the reason why under

these conditions the angular distances of the neutral points from the sun or antisun increase as the wavelength decreases. Then, the Arago, Babinet, Brewster and fourth neutral points are nearest the zenith or nadir in the blue; in the green they are positioned slightly further away from the zenith or nadir, and in the red their angular distance from the zenith or nadir is the greatest.

These features are more or less modified by wavelength-dependent reflection of light from the ground. If in a given spectral range the reflectivity of the ground is much higher than in other parts of the spectrum, in this spectral range the relatively greater amount of ground-reflected light alters strongly the skylight and earthlight polarization and the positions of the neutral points: If the ground-reflected light is horizontally (positively), vertically (negatively) polarized or unpolarized, it reduces, enhances or does not alter the area of negatively polarized region of the atmosphere around the sun and antisun, and therefore it decreases, increases or does not change the angular distance of the neutral points from the sun or antisun, respectively.

At sunset and sunrise, the spectral composition of direct sunlight changes considerably and the proportion of longer (yellow, orange, red) wavelengths increases. This phenomenon also changes the skylight and earthlight polarization as well as the neutral point positions. Similar effect occurs rarely after volcanic eruptions, when the wavelength-dependent absorption and scattering on the aerial particles of volcanic debris significantly modify the spectral composition of direct sunlight (Coulson 1988)

In the sky above the Tunisian desert, where the skylight polarization patterns in Figs. 7.3.1, 7.4.4 and plots of Figs. 7.4.5B,D,F and 7.4.6B,D,F were measured, the degree of skylight polarization was highest in the green rather than in the red. The reason for this anomaly is that the ground was reddish/yellowish sand, thus the amount of light reflected from the ground was largest in the red, which decreased the degree of skylight polarization in this part of the spectrum. This wavelength-dependent ground reflection and the reddish/orange direct sunlight at sunrise influenced also the positions of the Arago and Babinet points. The same phenomenon was observed by Horváth et al. (1998b) during the video-polarimetric study of the Arago point at sunset, at another place of the reddish Tunisian desert in 1996.

In the case of the air-borne observation of the Brewster and fourth neutral points, the characteristics and observability of both neutral points strongly depend on the altitude of the observer and the features of the underlying ground surface: Compared with the atmospheric contribution to polarized earthlight, the surface contribution is the smallest for the shorter (UV and blue) wavelengths and increases towards longer wavelengths. The higher the albedo of the surface in a given spectral range, the greater is the contribution of ground reflection to the polarized earthlight.

Under normal conditions, the four principal neutral points of atmospheric polarization are located in the solar vertical plane determined by the observer, the zenith/nadir and the sun. Depending on the meteorological conditions and the characteristics of the ground, at sunrise or sunset the Arago point and the fourth neutral point is positioned about  $20^\circ$  to  $30^\circ$  above and below the antisolar point,

respectively, while the Babinet and Brewster points are located  $20^\circ$  to  $30^\circ$  above and below the sun, but not necessarily mirror symmetrically. Under normal atmospheric conditions, from the ground only two of the four are visible at a given time, as the fourth neutral point is always below the horizon and the Arago point sets below the horizon at the same time the Brewster point appears above the horizon, and *vice versa*. The Babinet point is visible from before sunrise until after sunset. The Babinet and Brewster points as well as the Arago and fourth neutral points move closer to the sun and antisun, respectively, as the sun rises higher in the sky, merging into a single neutral point coincident with the sun and antisun when the sun reaches the zenith. The fourth neutral point can be observed only at higher altitudes ( $>$  about 900 m) from balloons, aircrafts or satellites, but not from higher mountains, because the shadow of mountains excludes direct sunlight from the region of the atmosphere below the antisun.

The Arago point has been observed more frequently than the Babinet or Brewster point, because its location in the portion of the sky with relatively small  $I$  and high  $p$ , opposite the sun makes it the easiest of the four to observe, and also since its position has been found to be more sensitive to the effects of atmospheric turbidity than the position of either the Babinet or Brewster point. While the Babinet point is also readily observed by visual means, the Brewster point is embedded in the brightest and least polarized region of the sky, and is therefore difficult to observe visually.

#### **7.4.7 Why the Fourth Neutral Point has not been Observed in Previous Air- or Space-Borne Polarimetric Experiments?**

In the past, several air-borne (balloon- or aircraft-borne) and space-borne polarimetric measurements have been performed, which could have been able to observe the fourth neutral point. Thus, it is rather surprising why has not been given any explicit, definite experimental evidence for the existence of this neutral point until the measurements of Horváth et al. (2002b). The reasons are manifold:

1. Earthlight contains a significant component due to scattering by the atmosphere, beside that due to surface reflection. For remotely sensed surface characterization and discrimination, however, such atmospheric contamination of the radiation field have generally been minimised or corrected for by use of radiative transfer models applicable to the conditions of observation. Since the polarization of sunlight due to atmospheric scattering is responsible for the origin of neutral points, the fourth neutral point had only little chance to be observed in air- or space-borne remote sensing measurements in which the atmospheric component of earthlight was minimised or corrected for to promote the observation of surface features.
2. The first attempt to measure the polarization of earthlight was done by Rao (1969): His balloon-borne measurements, performed over the White Sands area (New Mexico), exhibited depolarization of the Rayleigh scattering by a Lambertian ground, thus the fourth neutral point was not observable.

3. The first extensive measurements of earthlight polarization have been done during four Space Shuttle missions, and a preliminary presentation has been made by Coulson et al. (1986). Photographs were taken about the earth surface with a pair of cameras, each of which containing a linearly polarizing filter with different orientation of the transmission axis. Some qualitative data could have been deduced from the comparison of these polarizational picture pairs. Since for a complete imaging polarimetry three polarizational pictures are needed, the method used by Coulson et al. (1986) was inappropriate for the space-borne observation of the fourth neutral point.
4. Herman et al. (1986) performed a balloon-borne experiment to measure  $I$  and  $p$  of sunlight scattered by the stratospheric aerosol at near-infrared (850 and 1650 nm) wavelengths at an altitude of 20 km. Since only circular scans were done in a nearly ( $\pm 0.1^\circ$ ) horizontal plane with a narrow ( $2^\circ$ ) field-of-view point-source polarimeter when the sun was just at the horizon, the fourth neutral point, located at sunrise or sunset about  $20^\circ$ - $30^\circ$  below the antisun, could not have been investigated with this polarimeter.
5. Using the polarimetric device of Herman et al. (1986), Deuzé et al. (1989) performed a balloon-borne experiment for directional observations of  $I$  and  $p$  of earthlight. This apparatus with a  $2^\circ$  field of view has been adapted to polarimetric measurements at near infrared (850 and 1650 nm) wavelengths scanning in a vertical plane. A sun pointer allowed the gondola of the balloon to be stabilized at a given azimuth, thus polarimetric measurements have been done in a vertical plane which departed from the sun's/antisun's vertical plane by about  $8^\circ$ . In vertical scans at altitudes 28-31 km there were two local minima of  $p$  of earthlight [Deuzé et al. 1989, page 98, plot  $P(\theta)$  of sequence a) in Fig. 4]: one minimum in forward scattering (about  $25^\circ$  below the sun), and another minimum in backward scattering (about  $25^\circ$  below the antisun). The former and the latter minimum of  $p$  was observed near the Brewster point and the fourth neutral point, respectively. If the plane of the scan would have been exactly the sun's/antisun's vertical, Deuzé et al. (1989) could have observed as first the fourth neutral point.
6. The POLDER instrument (see Chapter 4), a space-borne imaging polarimeter, was designed to measure the directionality and polarization of the solar radiation scattered by the earth-atmosphere system (Deschamps et al. 1994). Three of the channels (443, 670, 865 nm) measured the linear polarization of the earthlight yielding the Stokes parameters  $I$ ,  $Q$ ,  $U$ , from which the total radiance  $L = I$ , the linearly polarized radiance  $L_{pol} = p \cdot L = (Q^2 + U^2)^{1/2}$ , and the angle of polarization  $\alpha$  were deduced. The POLDER-team prefers to use  $L_{pol}$  which is nearly additive with respect to the contributions of molecules, aerosols and land surfaces, rather than  $p$  in which polarized and unpolarized light are mixed ambiguously. Thus, in the publications of the POLDER-team colour-coded maps of  $L$  and  $L_{pol}$  have been used (see e.g. Fig. 6 of Deuzé et al. 1993, p. 145). Neutral points along the antisolar meridian, above and below the antisun never show up explicitly in the POLDER maps of  $L_{pol}$ . In these pictures, around the antisun there is usually an extended circular or elliptic dark grey or black spot (see Fig. 4.1C) representing zero and very low values of  $L_{pol}$  at all

three (443, 670, 865 nm) wavelengths. Farther away from the antisun, the picture gradually becomes more brighter and the colour more bluish because of the gradually increasing  $L_{pol}$  especially in the blue (443 nm) due to molecular (Rayleigh) scattering. At a given wavelength,  $L_{pol}$  is zero at the Brewster and fourth neutral point, the position of which depends on wavelength (Fig. 7.4.3, Table 7.4.1). These neutral points show up strikingly in the map of  $p$  measured at any wavelength, if very low  $p$ -values (0%, 1%, 2%, 3%, ...) are coded and visualized by strongly contrasting colours. In the maps of  $L_{pol}$  used by the POLDER-team, three coloured dark (almost black) spots should be seen at the positions of the Brewster and fourth neutral point at the three (443, 670, 865 nm) wavelengths. These dark coloured spots are, however always merged into the great dark spot around the antisun, since the zero and the very low values of  $L_{pol}$  are coded practically by the same very dark grey shades. On the other hand, the information available in the angle of polarization  $\alpha$  was practically not used by the POLDER-team; we do not know any published  $\alpha$ -map measured by the POLDER instrument.

7. Using the Mie theory, Bréon et al. (1997) computed the polarized phase function  $q(\gamma)$  for twelve different aerosol models as a function of the scattering angle  $\gamma$ .  $q(\gamma)$  is the product of the phase function and  $p$ . In their model they used different size distributions and refractive indices of the aerosol particles.  $q(\gamma)$  is negative when the direction of polarization is parallel to the plane of scattering and positive when it is perpendicular. Where the polarized phase function switches from negative to positive [ $q(\gamma^*) = 0$ ] there is a neutral point. Depending on the model parameters, in the twelve  $q(\gamma)$  plots computed by Bréon et al. (1997, p. 17188, Fig. 1b)  $q(\gamma^*) = 0$  for different scattering angles  $\gamma_1^*$  and  $\gamma_2^*$  where  $10^\circ < \gamma_1^* < 55^\circ$  and  $120^\circ < \gamma_2^* < 170^\circ$ . The neutral point at  $\gamma_1^*$  and  $\gamma_2^*$  corresponds with the Brewster and the fourth neutral point, respectively. Although from these numerical calculations a neutral point of earthlight polarization below the antisun can be deduced and predicted, in their numerous publications the POLDER-team never noted explicitly the existence of this neutral point and did not mention that it may correspond to the fourth principal neutral point. The most which was noted by Deuzé et al. (1993, pp. 144-145) is that around scattering angle "150° the polarized reflectance equals the molecular one. It shows that the aerosols exhibit zero polarization for a 150° scattering angle. For larger scattering angles, the aerosol polarization seems to increase again, with the polarization direction now parallel to the scattering plane ..."

According to their publications, the fourth as well as the Brewster neutral point have escaped the attention of the POLDER-team. Obviously, they used the polarization data collected by the POLDER instrument for practical, applied meteorological purposes. Nevertheless, the polarization data sensed remotely by the air-borne as well as space-borne versions of the POLDER instrument should latently contain the fourth neutral point of the normal clear sunlit atmosphere: It should have been calculated the  $p$ - and  $\alpha$ -maps measured at the three (443, 670,

865 nm) wavelengths and visualized in a format similar to that presented in this chapter.

#### 7.4.8 Concluding Remarks

One can conclude that the results of the two balloon-borne imaging polarimetric measurements of Horváth et al. (2002b) provided the first experimental/observational evidence for the existence of the fourth principal neutral point within the clear sunlit atmosphere. The fourth neutral point was observed from different altitudes between 900 m and 3500 m during and immediately after sunrise at the theoretically predicted position, at about  $22^{\circ}$ - $40^{\circ}$  below the antisun along the antisolar meridian, depending on the wavelength. The fourth neutral point has similar characteristics as the Arago, Babinet and Brewster points:

- It is located along the antisolar meridian at the edge of the areas of positive and negative polarization of earthlight.
- At sunrise, it is about at the same angular distance below the antisun as the Brewster point is below the sun.
- Its nadir angle decreases with decreasing wavelength.
- Its position and the polarizational characteristics of earthlight around it are influenced by ground reflection, the effect of which decreases as the altitude increases and/or the wavelength decreases.
- Its nadir angle is decreased by multiple scattering on atmospheric aerosols increasing the areas of negative polarization of earthlight.

The first balloon-borne observations by Horváth et al. (2002b) on the fourth neutral point are consistent with the earlier ground-based observations on the Arago, Babinet and Brewster points performed with video polarimetry (Horváth et al. 1998b; Horváth and Wehner 1999) or with full-sky imaging polarimetry (Gál et al. 2001a,b,c; Pomozi et al. 2001a,b; Horváth et al. 2002a, 2003). The fourth neutral point was not observed during earlier air- or space-borne polarimetric experiments and/or it escaped the attention of researchers, because

- some of these measurements were performed at longer (red or infrared) wavelengths in order to minimize the contribution of molecular scattering at shorter (UV and blue) wavelengths;
- the previous techniques were not adequate to measure neutral points;
- the routinely used non-imaging point-source scanning polarimeters were not pointed towards the fourth neutral point;
- unpolarized points did not show up explicitly in the polarization maps due to an inadequate, disadvantageous colour coding and displaying of the measured polarization data.

According to Coulson (1988, p. 242), more attention has been paid to the measurement of the positions of the Arago, Babinet and Brewster points than to any other feature of skylight polarization. This statement is now rounded off by the first observation, visualization and characterization of the fourth neutral point reported by Horváth et al. (2002b) 193 and 162 years after the discovery of the Arago point and the Babinet point, and 160 years following the first observation of the Brewster point.

## Table

**Table 7.4.1.** The angular distance of the Arago, Babinet, Brewster and fourth neutral points from the nadir or the zenith as determined on the basis of the patterns of the degree and angle of linear polarization measured at 650, 550 and 450 nm at different altitudes  $A$ . (After Table 1 of Horváth et al. 2002b, p. 2092).

neutral point	skylight						earthlight					
	Arago (from zenith)			Babinet (from zenith)			Brewster (from nadir)			fourth (from nadir)		
spectral range	650 (nm)	550 (nm)	450 (nm)	650 (nm)	550 (nm)	450 (nm)	650 (nm)	550 (nm)	450 (nm)	650 (nm)	550 (nm)	450 (nm)
$A = 3500$ m	—	—	—	—	—	—	56.3°	51.1°	46.6°	65.3°	49.8°	49.2°
$A = 1340$ m	—	—	—	—	—	—	53.4°	50.2°	53.4°	55.6°	56.9°	54.0°
$A = 900$ m	—	—	—	—	—	—	62.4°	62.4°	62.4°	55° ± 5°	55.3°	57.9°
$A = 0$ m	70.7°	64.4°	68.1°	59.0°	61.6°	65.5°	—	—	—	—	—	—

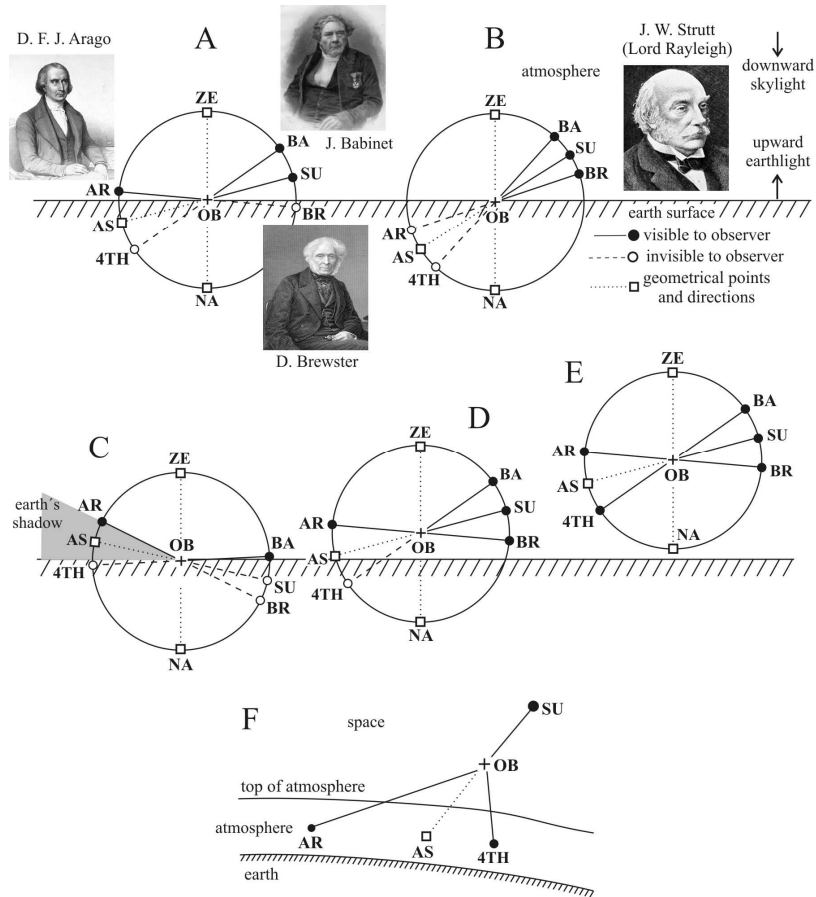


**Fig. 7.4.1.** A, B: Schematic diagram of the normal positions of the Arago (AR), Babinet (BA) and Brewster (BR) neutral points of skylight polarization in the vertical plane including the ground-based observer (OB), sun (SU), zenith (ZE), antisolar point (AS), and nadir (NA). From the ground, only two neutral points are visible simultaneously: either the Arago and Babinet points (A, for lower solar elevations), or the Babinet and Brewster points (B, for higher solar elevations). From the ground, the fourth neutral point (4TH) is not visible. The insets represent the portraits of Dominique Francois Jean Arago (1786-1853), Jacques Babinet (1794-1872) and David Brewster (1781-1868), the discoverer of the neutral points. The portrait of John William Strutt, alias Lord Rayleigh (1842-1919) who developed the first theory of skylight polarization, is also shown as an inset. C: The fourth neutral point cannot even be observed after sunset, because the atmosphere below the antisun is then in the shadow of the earth. D: Increasing the altitude of observation, above a certain height three neutral points can be observed simultaneously: the Arago, Babinet and Brewster points. E: At an appropriately high altitude, all four neutral points can be observed simultaneously. Then, the Arago and Babinet points are the neutral points of downwelling polarized skylight, while the Brewster and fourth neutral points are the neutral points of upwelling polarized earthlight. F: Geometry of the space-borne observation of the Arago and fourth neutral points. (After Fig. 1 of Horváth et al. 2002b, p. 2086).

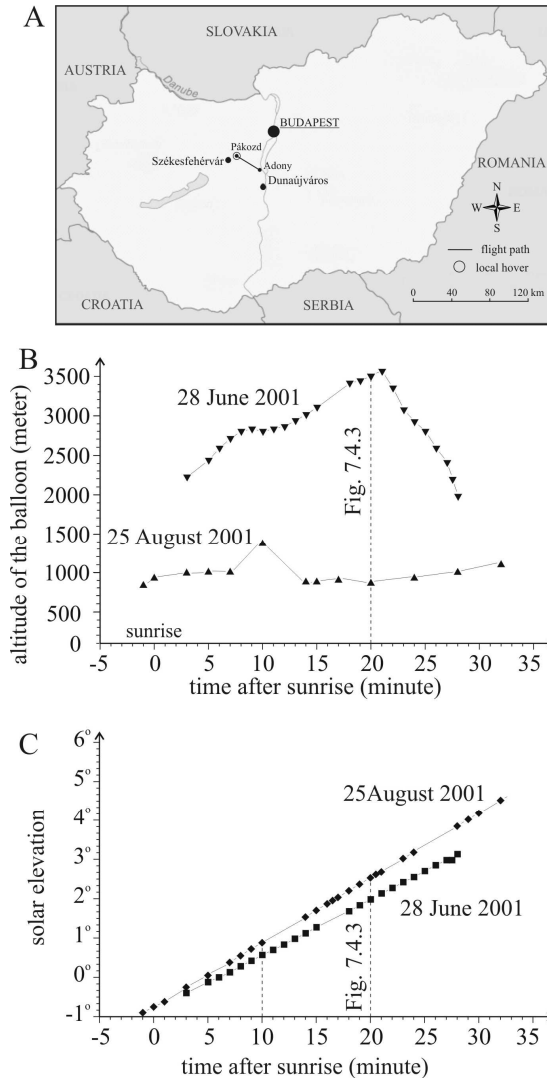


**Fig. 7.4.2.** Main parameters of the two hot air balloon flights of Horváth et al. (2002b) conducted on 28 June (local sunrise at 04:52 = local summer time = universal time code + 2 = UTC+2) and 25 August (sunrise at 05:56) 2001 to measure the polarization patterns of upwelling earthlight and the characteristics of the fourth neutral point of atmospheric polarization. A: The launching site (Pákozd, 47°13'N, 18°33'E), landing site (Adony, 47°06'N, 18°51'E) and trajectory of the first flight (hovering above the launching site during the second flight) on the map of Hungary. B, C: Altitude of the balloon and solar elevation as a function of time after sunrise for both flights. In graph B the black-filled triangles represent the altitudes and points of time at which polarimetric measurements were done. In both plots a dashed vertical line marks the time of the measurement, the results of which are shown in Fig. 7.4.3. (After Fig. 2 of Horváth et al. 2002b, p. 2088).

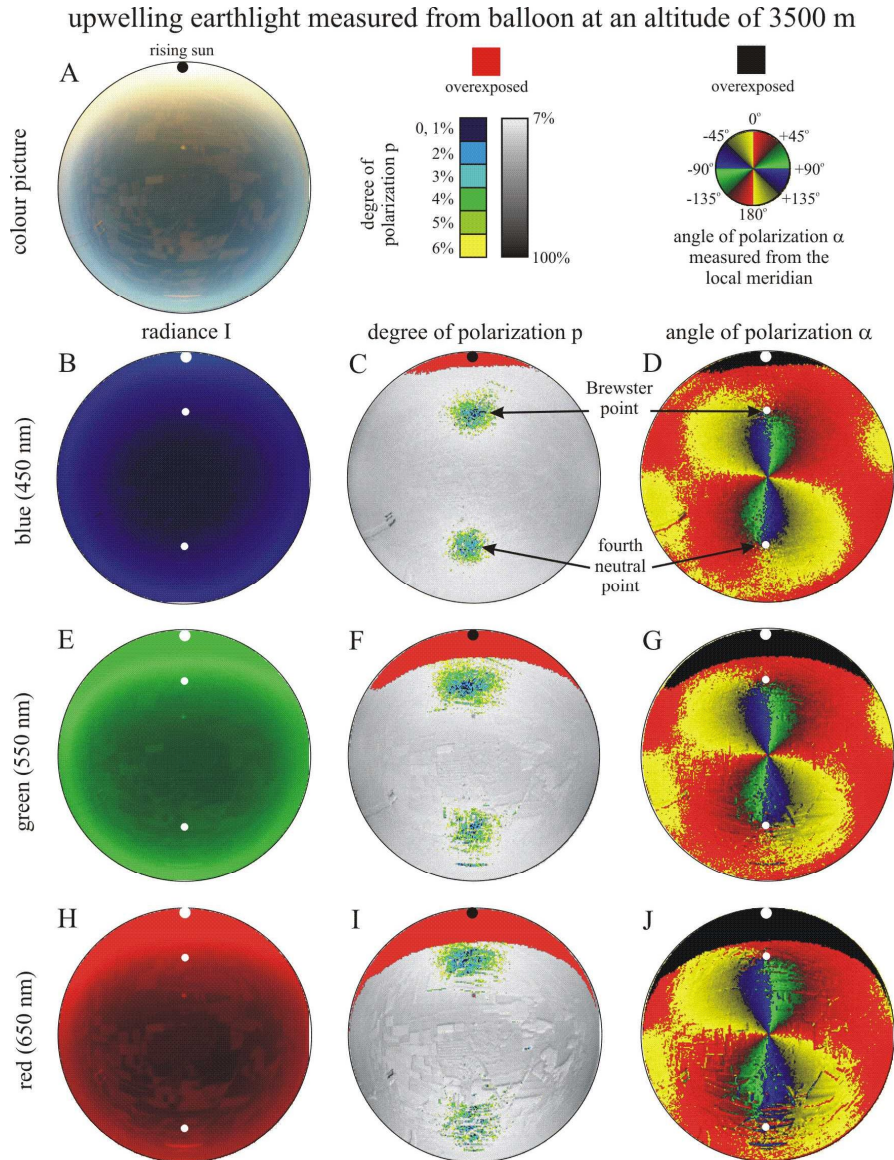


**Fig. 7.4.3.** 180° field-of-view photograph of the landscape below the gondola of the hot air balloon (A) and the patterns of radiance  $I$  (B, E, H), degree of linear polarization  $p$  (C, F, I) and angle of polarization  $\alpha$  (D, G, J) of upwelling earthlight. Measurements were taken by using 180° field-of-view imaging polarimetry at an altitude of 3500 m and a solar elevation of 2° at 450, 550 and 650 nm immediately after local sunrise (05:12; local summer time = UTC+2; 28 June 2001). The position of the sun and the neutral points are indicated by dots. Time of exposure = 1/60 s, aperture = 2.8, colour reversal film: Fujichrome Sensia II, 100 ASA. (After Fig. 4 of Horváth et al. 2002b, p. 2090).

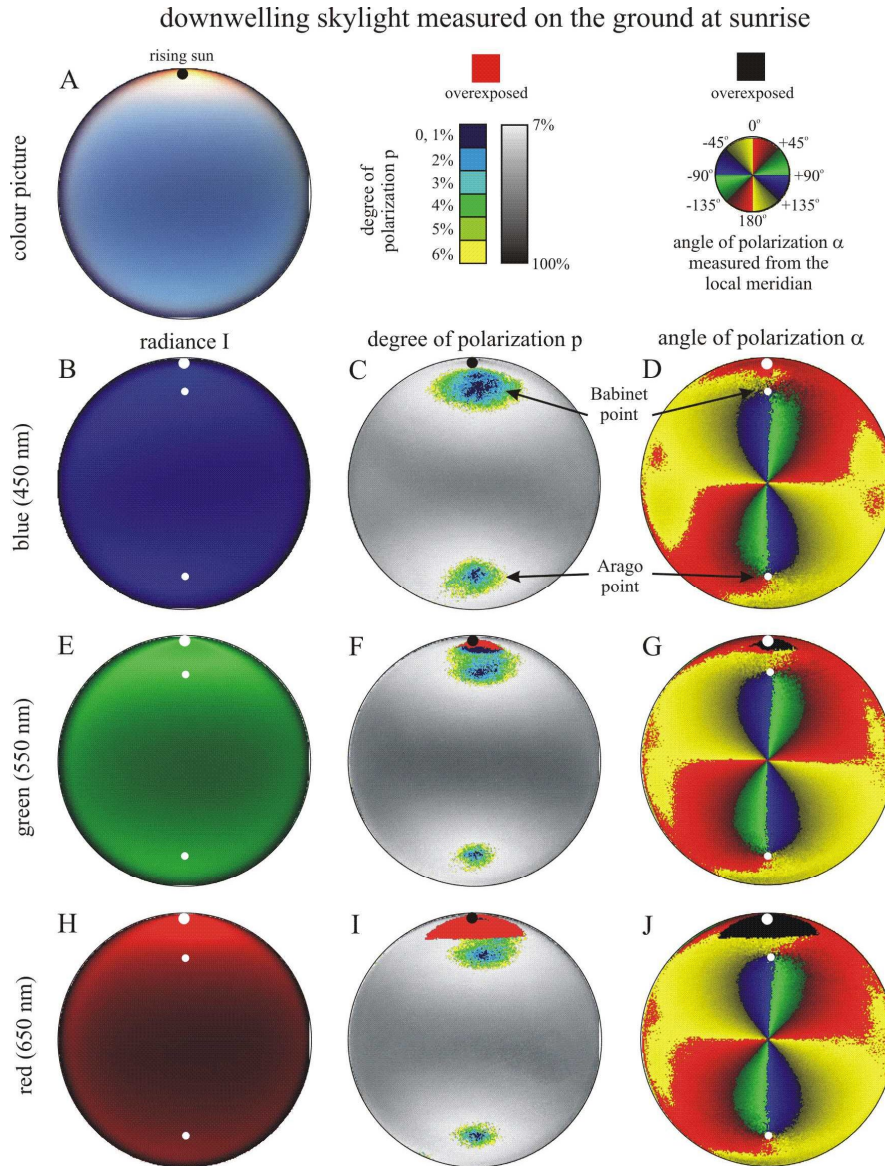


**Fig. 7.4.4.** As Fig. 7.4.3 for the full clear sky measured from the ground at local sunrise (26 August 1999, 06:00 = local summer time = UTC+1, solar elevation =  $0^\circ$ ; salt pan Chott el Djerid, 10 km from Kriz,  $33^\circ 52'N$ ,  $8^\circ 22'E$ , Tunisia). Note that on the compass rose East and West are transposed, because we are looking up towards the celestial dome rather than down towards the ground. Time of exposure =  $1/60$  s, aperture = 2.8, using Fujichrome Sensia II 100 ASA colour reversal film as detector. (After Fig. 5 of Horváth et al. 2002b, p. 2093).

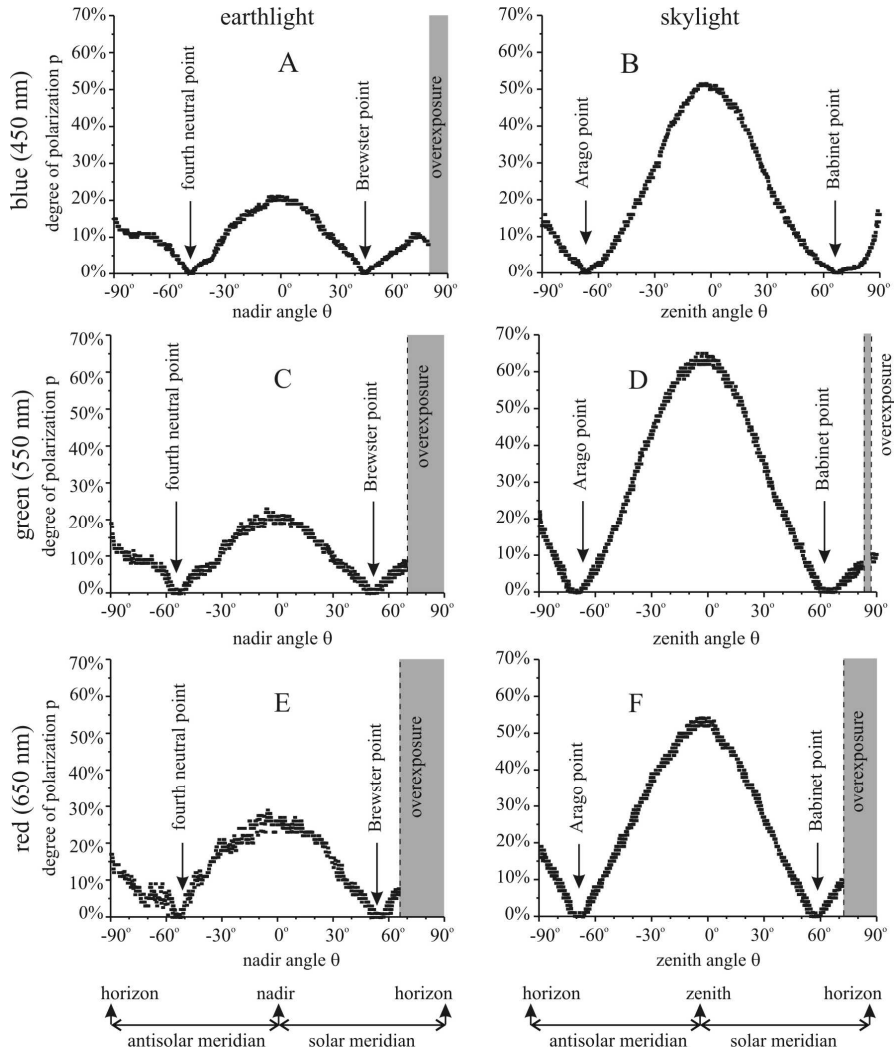


**Fig. 7.4.5.** Degree of linear polarization  $p$  of earthlight (A, C, E) and skylight (B, D, F) along the solar and antisolar meridian measured at 450, 550 and 650 nm as a function of the nadir/zenith angle  $\theta$ . Data for earthlight and skylight originate from the polarization patterns in Figs. 7.4.3 and 7.4.4, respectively. Grey stripes show the overexposed areas. (After Fig. 6 of Horváth et al. 2002b, p. 2094).

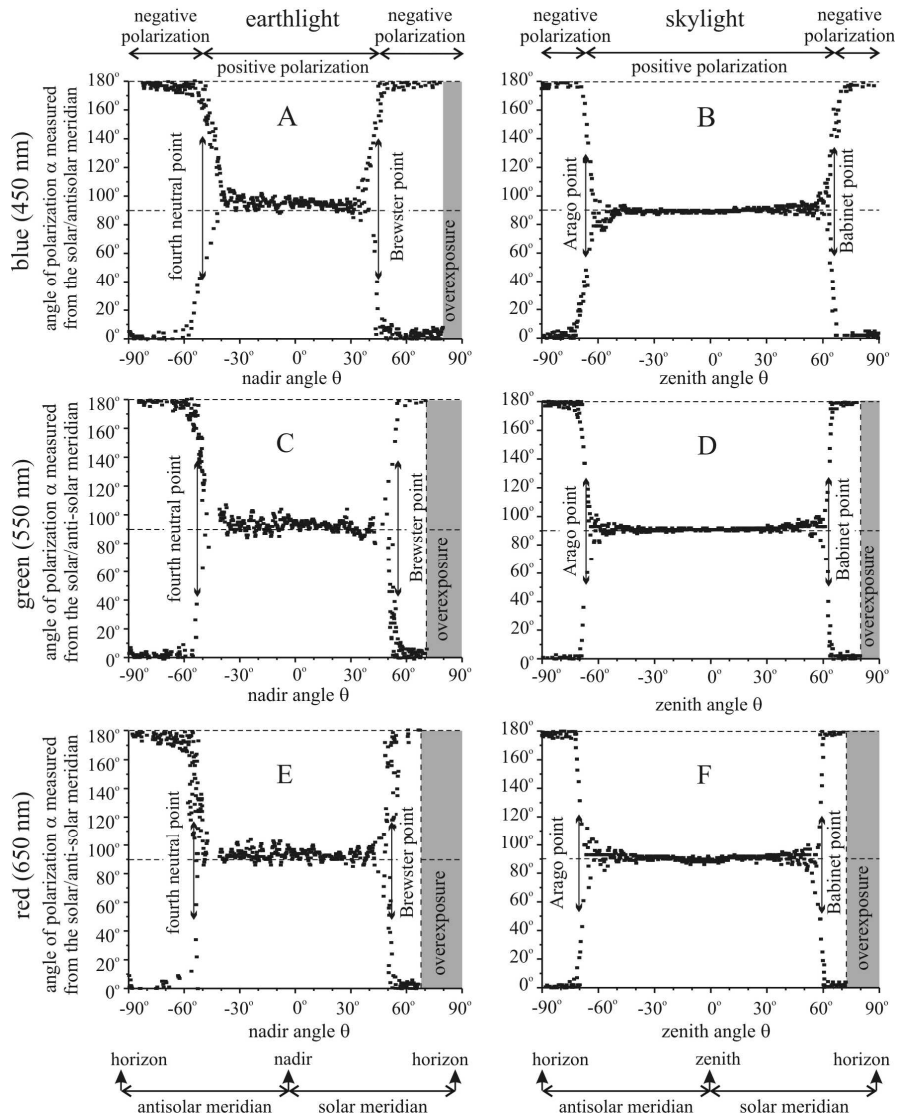


**Fig. 7.4.6.** As Fig. 7.4.5 for the angle of polarization  $\alpha$  of earthlight and skylight measured from the solar/antisolar meridian. (After Fig. 7 of Horváth et al. 2002b, p. 2095).

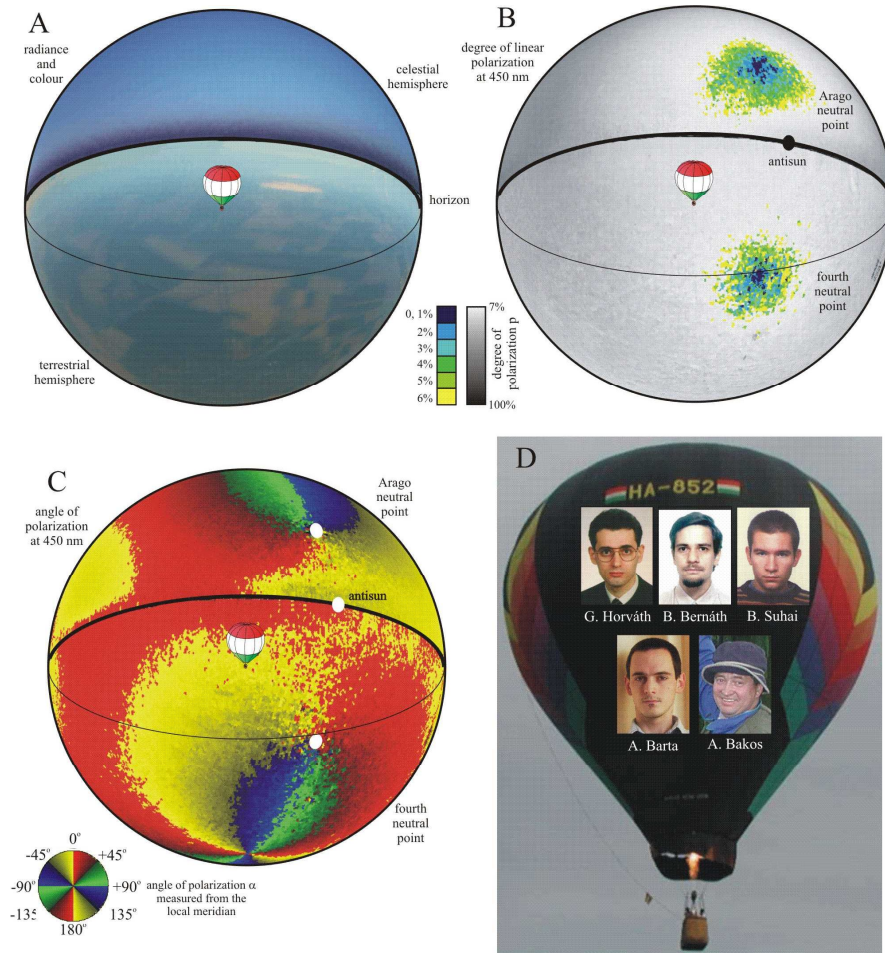


**Fig. 7.4.7.** Perspectivic representation of the three-dimensional spatial distribution of radiance and colour (A), degree (B) and angle (C) of linear polarization as well as the Arago and fourth neutral points on the surface of spheres. Similar patterns can be observed/measured around a hot air balloon in the blue (450 nm) spectral range at an altitude of 3500 m. Every sphere in the picture is the combination of the patterns in Figs. 7.4.3A,C,D and 7.4.4A,C,D. D: Portraits of Gábor Horváth, Balázs Bernáth, Bence Suhai and András Barta, who observed as first the fourth neutral point during two hot air balloon flights, the pilot of which was Attila Bakos. (After Fig. 8 of Horváth et al. 2002b, p. 2096).